Coding errors in the Pathfinder AVHRR Land (PAL) data set's atmospheric correction algorithm

The following material has been abstracted from a memorandum written by Dr. Satya Kalluri (UMD, Dept. of Geography) describing his PAL validation support findings.

Coding errors in the Rayleigh and ozone correction algorithm

In July 1994, the Pathfinder calibration/atmospheric correction software was thoroughly examined as a part of the software development activities. A detailed examination of the code revealed that two of the parameters which are being supplied to the users are not derived exactly as described in the user's manual. The two problems identified in the processing are:

1. The visible and near IR reflectances from AVHRR channels 1 and 2, respectively, which are provided with the Pathfinder HDF data files have **not** been normalized for the variations in solar zenith angle.

2. The corrections for Rayleigh scattering and ozone absorption in the atmosphere, for which channels 1 and 2 are corrected, have been underestimated.

   Details of the coding errors are given in Appendix 1.

APPENDIX-1

Atmospheric Correction Algorithm Details

The Pathfinder processing algorithm is designed to correct channel 1 and 2 reflectances for the ozone absorption and Rayleigh scattering in the atmosphere following Gordon et al. 1988. The apparent radiation reaching the sensor from the ground after attenuation by ozone absorption and Rayleigh scattering in the atmosphere can be described by (Gordon et al. 1983):

$$L(\theta_s, \theta_v, \varphi) = L_r(\theta_s, \theta_v, \varphi) + T \bullet L_s(\theta_s, \theta_v, \varphi) \qquad (1)$$

where

L is the calibrated radiance observed by AVHRR in channel 1 and 2 above the atmosphere (Watts/m^2 μm sr)

θ_s is the solar zenith angle

θ_v is the view zenith angle

φ is the relative azimuth between the sun and the satellite vertical planes

L_r is the upward radiance caused by Rayleigh scattering (Watts/m^2 μm sr)

T is the diffuse transmission of the atmosphere between the surface and the sensor, and

$L_s(\theta_s, \theta_v, \varphi)$ is the radiance leaving the surface (Watts/m^2 μm sr)

Equation 1 can be expanded as

$$L(\theta_s, \theta_v, \varphi) = T_o \bullet \{L_r(\theta_s, \theta_v, \varphi) + T_r \bullet \frac{\mu_s F_o}{\pi} \bullet \frac{\rho_{o,r}(\theta_s, \theta_v, \varphi)}{1 - S_r \rho_{o,r}(\theta_s, \theta_v, \varphi)}\} \qquad (2)$$

where

T_r is the transmission function of atmosphere with Rayleigh scattering

μ_s is the cosine value of solar zenith angle

F_o is the solar spectral irradiance above the atmosphere with a unit of (Watts/m^2 μm)

$\rho_{o,r}(\theta_s, \theta_v, \varphi)$ is the surface directional reflectance with ozone and Rayleigh scattering corrections

S_r is the spherical albedo of the Rayleigh atmosphere

However, Equation 2 is approximated as:

$$L(\theta_s, \theta_v, \varphi) = T_o \bullet \{L_r(\theta_s, \theta_v, \varphi) + T_r \bullet \frac{\mu_s F_o}{\pi} \bullet \rho_{o,r}(\theta_s, \theta_v, \varphi)\} \quad (3)$$

It should be noted that while Equation 2 is an accurate description of the radiative transfer between the land surface and the sensor, Equation 3 is only an approximation. Equation 3 does not account for the multiple interaction between the surface and the atmosphere. While the multiple scattering between the surface and the atmosphere is negligible for most land surfaces, it is not the case when the land cover is very bright such as over ice and snow.

From Equation 3, $\rho_{o,r}(\theta_s, \theta_v, \varphi)$ can be estimated:

$$\rho_{o,r}(\theta_s, \theta_v, \varphi) = \frac{L(\theta_s, \theta_v, \varphi)\pi / \mu_s F_o - \left(L_r(\theta_s, \theta_v, \varphi)\pi / \mu_s F_o \right) \bullet T_o}{T_o \bullet T_r} \quad (4)$$

Following Gordon et al. (1983), the total transmission function for ozone (T_o) after two trips in the atmosphere is approximated as:

$$T_o = \exp(-\tau_o / \mu_s - \tau_o / \mu_v) \quad (5)$$

However, the optical depth of Rayleigh atmosphere is reduced by a factor of 2 due to diffuse transmission, and the Rayleigh transmittance is given by:

$$T_r = \exp(-\tau_r/2\mu_s - \tau_r/2\mu_v) \quad (6)$$

where τ_o, and τ_r are the optical thickness of ozone and Rayleigh in the atmosphere respectively, and μ_v is the cosine value of the satellite view angle. While τ_o is estimated from ozone measurements from the TOMS instrument, τ_r is defined as:

$$\tau_r = \tau_r^{'} \bullet \exp\left(-altitude/8434(\text{Atmospheric scale hight in meters})\right) \quad (7)$$

where $\tau_r^{'}$ is atmospheric optical thickness at the sea level, which has a constant value of 0.057 and 0.02 for channels 1 and 2 respectively. The exponential term on the right hand side of Equation 7 is an adjustment to account for the variations in Rayleigh optical thickness as a function of surface elevation.

L_r in Equation 3 is defined as:

$$L_r(\theta_s, \theta_v, \varphi) = F_o \bullet I(\theta_s, \theta_v, \pi - \varphi) \bullet \frac{1 - \exp(-\tau_r/\mu_v)}{1 - \exp(-\tau_r^{'}/\mu_v)} \quad (8)$$

where $I(\theta_s, \theta_v, \pi - \varphi)$ is proportional to radiance due to Rayleigh scattering in the atmosphere and is read from a lookup table generated by the University of Miami following Gordon et al. (1988).

Substituting (5), (6), (7) and (8) in Equation 4 we have:

$$\rho_{o,r}(\theta_s,\theta_v,\varphi)=\frac{\dfrac{\pi L_{(\theta_s,\theta_v,\varphi)}}{\mu_s F_o}-\dfrac{\pi}{\mu_s}\bullet I(\theta_s,\theta_v,\pi-\varphi)\bullet\dfrac{1-\exp(-\tau_r/\mu_v)}{1-\exp(-\tau_r'/\mu_v)}\bullet T_o}{T_o\bullet T_r} \qquad (9)$$

However, in the Pathfinder processing software the formula actually implemented for calculating the surface reflectance with ozone and Rayleigh scattering corrections was:

$$\rho_{path}=\frac{\dfrac{\pi L(\theta_s,\theta_v,\varphi)}{F_o}-I(\theta_s,\theta_v,\varphi)\bullet\dfrac{1-\exp(-\tau_r/\mu_v)}{1-\exp(-\tau_r'/\mu_v)}\bullet T_o}{\exp(-\tau_r/\mu_s-\tau_r/\mu_v)\bullet\exp(-\tau_o/\mu_s)} \qquad (10)$$

It is the differences in these two equations (9 and 10) which are the basis of the errors in the atmospheric correction algorithm. The implications of these errors are:

1. The differences in NDVI derived from channels 1 and 2 before and after normalization for solar illumination are very small (less than 0.008 as illustrated in Figures 3a and 3b), and are caused only due to rounding errors beyond the third decimal during the processing of NDVI. Users wishing to normalize the data for solar illumination can do so by dividing the reflectances in channels 1 and 2 by the cosine of the solar zenith angle (in degrees). Solar zenith angle values are provided along with the data set for each pixel (in the HDF files).

2. As stated above, the correction for Rayleigh scattering and ozone absorption has been underestimated in channels 1 and 2. The magnitude of atmospheric correction varies as a function of satellite geometry and surface type. A pixel by pixel comparison of channel 1 and 2 reflectances from a sample of the Pathfinder global data set with reflectances derived after accurate correction showed root mean square differences (RMS*) of 3.24% absolute reflectance in

*RMS $= \left[\sum_i^N \left(\rho_{path}-\rho_{o,r}\right)^2 / N\right]^{1/2}$

channel 1 and 1.56% in channel 2 respectively. Figures 1 and 2 show the magnitude of underestimation in the atmospheric correction over two different targets with contrasting land cover. The RMS difference between the Pathfinder NDVI and the more accurately corrected NDVI was found to be 0.05. Table 1 shows the differences in channel 1 and 2 reflectances over two contrasting cover types before and after atmospheric correction from a sample of the data set. It can be seen from Table 1 that the differences in reflectance before and after Rayleigh and ozone correction are higher in channel 1 than in channel 2, and the over all increase in NDVI is generally higher in the back scatter direction than in the forward scatter direction. These results are consistent with those of Tanre et al. (1992).

3. The reflectances used in performing the CLAVR test **are** normalized for solar zenith angle variations with no Rayleigh or ozone corrections applied. However, the normalized top of the atmosphere reflectances used by CLAVR are not retained in the output data set.

Table 1

A comparison of channel 1 and 2 reflectances, and NDVI measurements before and after atmospheric correction over two contrasting cover types. The desert targets are in the Sahara, while the forest targets are over the Congo basin in Africa. These samples are from January 2, 1991.

Scan angle†	Cover type	channel 1 before correction (%)	channel 2 before correction (%)	NDVI before correction	channel 1 after correction (%)	channel 2 after correction (%)	NDVI after correction

where ρ_{path} is the reflectance from the original Pathfinder processing with an underestimation in Rayleigh and ozone correction, $\rho_{o,r}$ is the reflectance after an accurate correction, and N is the total number of pixels over land in the Pathfinder data set.

0	Desert	39.58	42.86	0.03	34.89	40.93	0.07
-35	Desert	27.08	24.28	-0.05	20.37	21.89	0.03
+35	Desert	42.03	41.33	-0.01	38.23	39.74	0.01
0	Forest	6.94	18.04	0.44	4.73	17.03	0.56
-35	Forest	12.54	27.14	0.36	7.68	25.06	0.52
+35	Forest	6.01	18.90	0.51	4.76	18.17	0.58

† Scan angles are in degrees. Positive numbers indicate forward scattering, and negative numbers indicate back scattering.

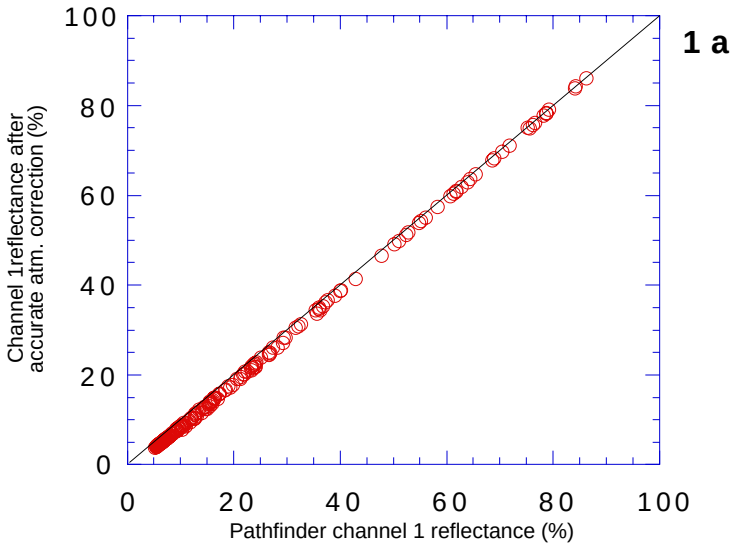

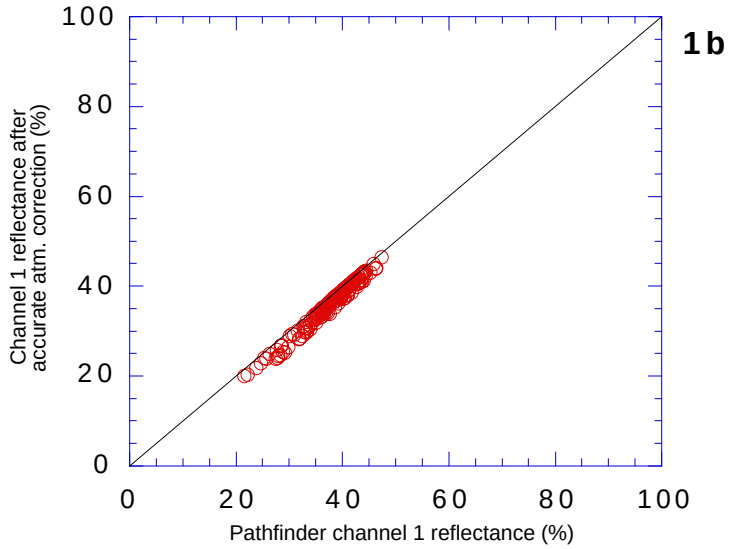

Figure 1. A comparison between channel 1 reflectances with accurate correction for Rayleigh and ozone, and the original Pathfinder reflectances (both the values have been normalized by the cosine of the solar zenith angle). Figure 1a is over the Amazon and Figure 1b is over the Sahara on January 2, 1991. No cloud screening has been applied to this data set.

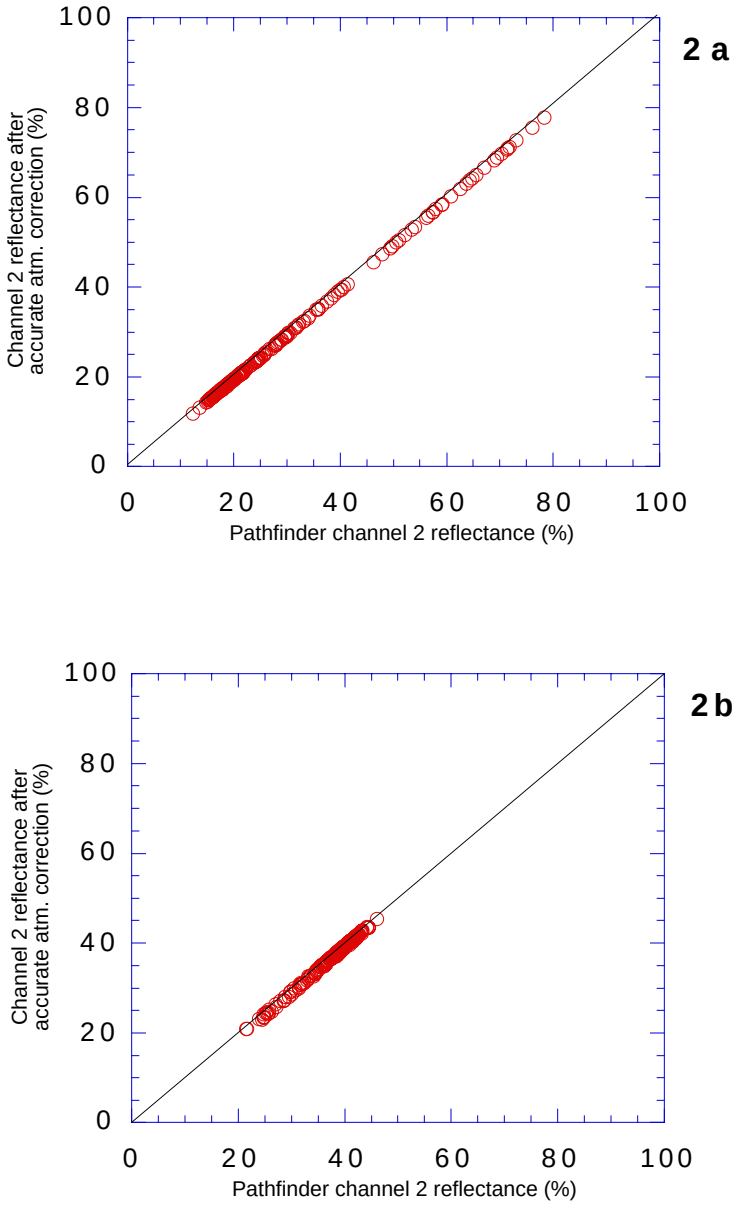

Figure 2. A comparison between channel 2 reflectances with accurate correction for Rayleigh and ozone, and the original Pathfinder reflectances (both the values have been normalized by the cosine of the solar zenith angle). Figure 2a is over the Amazon and Figure 2b is over the Sahara on January 2, 1991. No cloud screening has been applied to this data set.

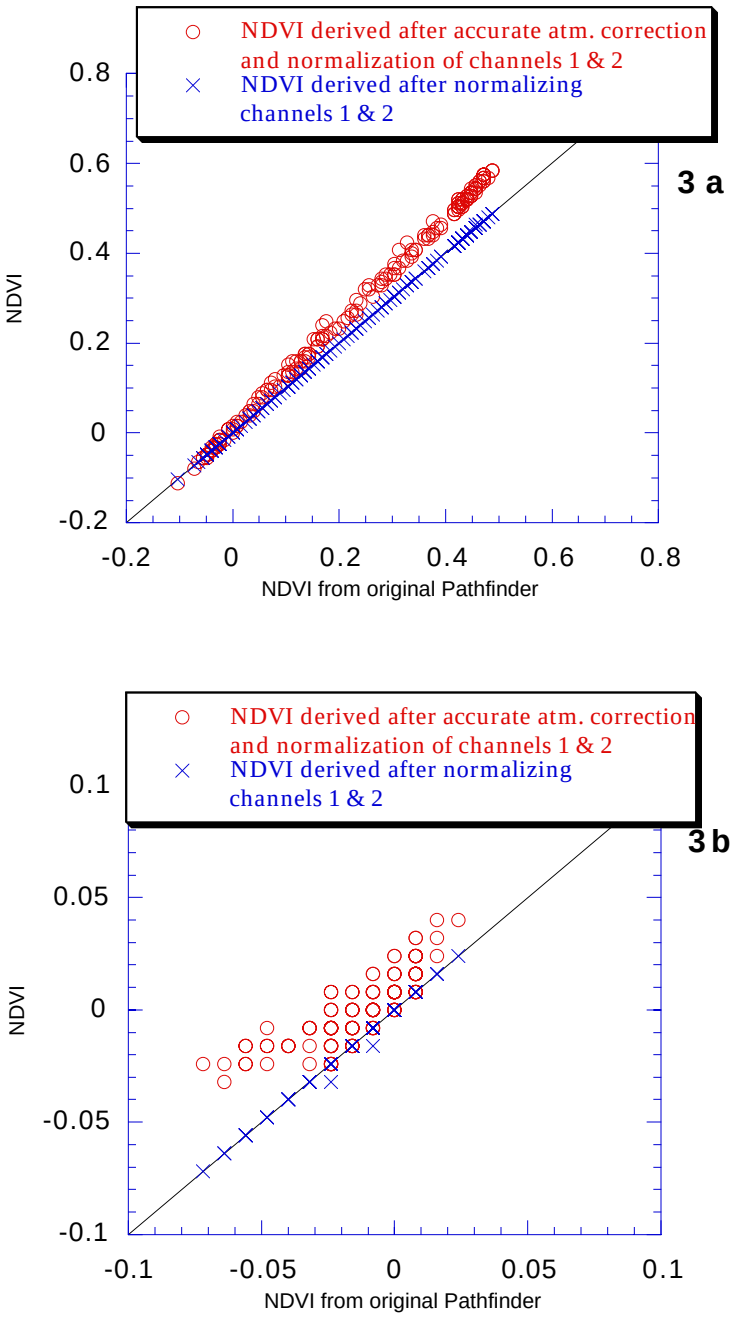

Figure 3. A comparison between NDVI derived from channels 1 and 2 with accurate correction for Rayleigh and ozone, and the original Pathfinder NDVI. Figure 3a is over the Amazon and Figure 3b is over the Sahara on January 2, 1991. No cloud screening has been applied to this data set.

References:

Gordon, H. R., J. W. Brown, and R. H. Evans, Exact Rayleigh scattering calculations for use with the Nimbus-7 Coastal Zone Color Scanner, *Applied Optics*, 27, 862-871, 1988.

Gordon, H. R., D. K. Clark, J. W. Brown, O. B. Brown, R. H. Evans, and W. W. Broenkow, Phytoplankton pigment concentrations in the middle Atlantic bight: comparison of ship determination and CZCS estimates, *Applied Optics*, 22, 20-36, 1983.

Tanre, D., B. N. Holben, and Y. J. Kaufman, Atmospheric correction algorithm for NOAA-AVHRR products: theory and applications, *IEEE Transactions on Geoscience and Remote Sensing*, 30, 231-248, 1992.